Lab on a Chip

RSC Publishing

PAPER

Attractive-repulsive dynamics on light-responsive chiral microparticles induced by polarized tweezers†

Cite this: *Lab Chip*, 2013, **13**, 459

Raúl Josué Hernández,[a] Alfredo Mazzulla,[b] Alfredo Pane,[b] Karen Volke-Sepúlveda[c] and Gabriella Cipparrone*[ab]

Received 21st June 2012,
Accepted 22nd November 2012

DOI: 10.1039/c2lc40703e

www.rsc.org/loc

Multifunctional colloidal micro and nano-particles with controlled architectures have very promising properties for applications in bio and nanotechnologies. Here we report on the unique dichotomous dynamical behaviour of chiral spherical microparticles, either fluid or solid, manipulated by polarized optical tweezers. The particles are created using a reactive mesogen mixed with a chiral dopant to form cholesteric liquid crystal droplets in water emulsion. The photopolymerization enables the chiral supramolecular configurations to be frozen in solid particles. Different internal architectures in the supramolecular structures, guided by the interfacial chemistry, enable optically isotropic or anisotropic spherical objects to be obtained. For particles having radial configuration of the cholesteric helices, we show that light can exert either a repulsive or attractive force depending on the handedness of its circular polarization, due to the unique selective reflection property of the cholesteric phase. On the other hand, very exotic dynamics is observed in the case of anisotropic chiral particles. Depending on the light handedness, they behave like Janus spherical particles with dissimilar optical properties, meaning that the surface of the dielectric particles is partly transparent and partly reflecting. We foresee interesting potential applications in micro and optofluidics, microphotonics and materials science.

1 Introduction

In 1970, when Arthur Ashkin performed the first experiment on guiding and trapping of microparticles by the forces of radiation pressure with a laser beam, a new and exciting scientific research area was initiated.[1] But the real breakthrough was in 1986, when Ashkin and coworkers demonstrated the single beam optical trap,[2] known at present as optical tweezers. Since then, a variety of particles have been optically manipulated, including purely dielectric, metallic, and biological particles *in vivo*, using different kinds of new traps and techniques.[3–9] This has led to considerable developments not only in physics, but also in biology and soft condensed matter.[10–16]

Micro-optofluidics and nanophotonics, such as optical trapping and manipulation, have developed from basic science into cutting-edge technologies in the past twenty years.[17,18] Recent advances, coming from the permutations and combinations of optics, photonics, and microfluidics, demonstrate how these fields are fast growing and still experiencing significant revolutions.[19–22] This is partly due to the number and diversity of influences, and partly due to the fact that mixing non-solid media with solid-state fluidic structures provides a nearly limitless range of combinations.

In this context, soft materials, such as liquid crystals (LCs), are an interesting example of systems that are easy to handle but also rich in complexity and capable of self assembly in a variety of supramolecular structures exhibiting high response functions. These features make LCs very appealing candidates for original applications in many areas, like colloidal systems, optical control, sensors, laser sources, optofluidics *etc.*[23–26] In fact, LCs are suitable materials for optical manipulation and transfer of optical angular momentum.[27–30] Due their high linear birefringence ($\Delta n \sim 0.2$), circularly polarized optical tweezers have been used to induce rotation of nematic LC droplets.[30–33] Particular attention has also been given to cholesteric liquid crystals (CLCs) for photonic applications.[25,26,34] This is because, besides linear anisotropy, chirality at supramolecular level is present in the cholesteric phase, where a helical configuration of the molecular director[23] is responsible for interesting properties, such as a 1D photonic band-gap for circularly polarized light travelling along the helical axis.

The geometrical confinement of LCs in micrometer-sized systems, like droplets, is a mean to obtain the formation of a range of thermodynamically stable molecular configurations exhibiting different topologies.[35,36] Moreover, the techniques used to induce specific ordering in LC layers by means of

[a]*Physics Department, University of Calabria, 87036 Rende-CS, Italy. E-mail: gabriella.cipparrone@fis.unical.it*
[b]*CNR-IPCF LiCryL Laboratory, 87036 Rende-CS, Italy*
[c]*Instituto de Física, UNAM, Apdo. Postal 20-364, 01000 México D.F., México*

† Electronic Supplementary Information (ESI) available: Movies 1–5. See DOI: 10.1039/c2lc40703e

surfaces and contaminants have been adopted in LC emulsion to produce a large variety of LC droplets.[28,37] In the particular case of CLCs, the droplets exhibit complex confined geometries that reflect how the molecules orientation at the interface with the surrounding medium influences the arrangement of the helicoidal super-molecular structures.[35,36] Recently,[38] we demonstrated that the use of reactive mesogens, instead of low mass molecular LCs, enables freezing of the LC droplets in solid particles with physical properties connected to their internal configuration. Moreover, adding proper photoluminescent dyes to the LC mixture, the solid microparticles can be used as microcavities to create 3D microlasers.[38]

With all the possibilities of tailoring the photonic properties of these chiral microparticles, their optical control can lead to exciting new architectures of optically driven sensors and components for microfluidics applications. Nevertheless, up to now only few works on the optical manipulation of chiral objects have been reported in the literature.[39–41]

In the present work, we investigate and demonstrate the unique optical manipulation features of different kinds of chiral spherical microparticles (fluid and solid) by means of circularly polarized optical tweezers. The ability to manipulate the internal arrangement of the LC droplets by controlling the chemical properties of the surrounding medium, as described in section 2, gives spherical particles that, depending on the helical internal configurations, become either optically isotropic or anisotropic chiral objects; we study both kinds of particles. The results of the optical manipulation experiments are described in section 3, and discussed in terms of the isotropy or anisotropy of the different particles. As we shall see, with proper light wavelength, an isotropic particle, having a radial configuration of the internal helical structures, can be either attracted by or repelled from the optical trap depending on the handedness of the circular polarization. This dynamic has been never reported before, to the best of our knowledge. Due to the isotropy of the particle, its qualitative behaviour in the optical trap can be understood, in the first instance, with a ray tracing model. On the other hand, the optical anisotropic particles, with conical or cylindrical configurations of the helical structures, exhibit an unusual dynamics as well. They behave like Janus particles with two dissimilar surface transmission properties, responsible of a very complex motion. Our findings are summarized and discussed in terms of perspectives of new applications in the last section.

2 Sample preparation and experiments

The CLC is obtained by dissolving chiral molecules in a nematic LC. The nematic phase is obtained using the reactive mesogen contained in RMS03-001C solution by Merck, Germany. The pure reactive mesogen was separated from the solvent PGMEA (propylene glycol monomethyl ether acetate) in the RMS03-001C using vacuum evaporation at 90 °C overnight. Then it was mixed with left-handed chiral dopant ZLI-811 (Merck, Germany, ~25% wt).

As it is well known, the molecular structure undergoes a helical distortion, *i.e.* spatial twisting of the molecules perpendicular to the director. The obtained helix might be right-handed or left-handed (according with the choice of chiral dopant) and is characterized by the helical pitch p, defined as the distance over which the local molecular director rotates by 2π. When CLC samples are aligned with their helicoidal axis parallel to the direction of the incident light, a wavelength band is selectively reflected due to the Bragg reflection.[23] The selectively reflected wave is circularly polarized with the same handedness of the cholesteric helix. On the contrary, light with the same wavelength but opposite circular polarization is transmitted through the cholesteric helix practically unchanged[23] (Fig. 1a).

The central wavelength λ_o and the spectral width $\Delta\lambda$ of the reflected light are related to the cholesteric pitch p, the average refractive index and the optical anisotropy Δn of the material:

$$\lambda_o = p\frac{(n_{II}+n_{\perp})}{2} \quad (1)$$

and

$$\Delta\lambda = p\Delta n \quad (2)$$

where $\Delta n = n_{II} - n_{\perp}$, n_{II} and $n_{\perp}$ being the refractive indices parallel and perpendicular to the molecular director, respectively. To illustrate this behaviour, the optical transmission spectrum of a planar thin film of the polymerized CLC measured when linearly polarized light impinges on it is shown in Fig. 1b. The reflection band was detected by optical transmission spectroscopy and the bandwidth is related to the pitch by eqn (2). In reflection mode, the selective reflection was directly observed through the colour of the cell, shown in the inset of Fig. 1b.

The CLC droplets emulsions were prepared by adding pure water to obtain a 0.5% wt concentration of the chiral active mesogen. Shaking the suspensions at 35 Hz and 60 °C for one minute in a laboratory vortex mixer, emulsions of spherical droplets with diameters (d) between 1 and 30 μm were obtained. The CLC droplets take a spherical shape and a parallel orientation of the LC molecules occurs at the water interface due to the LC hydrophobicity. The microscope observations in transmission mode between crossed polarizers (Fig. 2a) show the typical cross pattern of an optically isotropic droplet; while the observations in reflection mode, reported in ref. 38, show a central coloured spot that is independent of the particle orientation (*i.e.* omnidirectional selective reflection). These microscope investigations reveal the radial configuration of the helical axes, corresponding to an isotropic geometry of the helicoidal structures inside the particles, as reported in Fig. 2d.

On the other hand, the addition of a surfactant (cleaning compound Ausilab 300 from Carlo Erba, 0.02%wt) in the water emulsion promotes perpendicular anchoring of the LC molecules at the interface, as a consequence, the CLC droplets self-organize in different internal configurations. The microscope observation in transmission mode between crossed

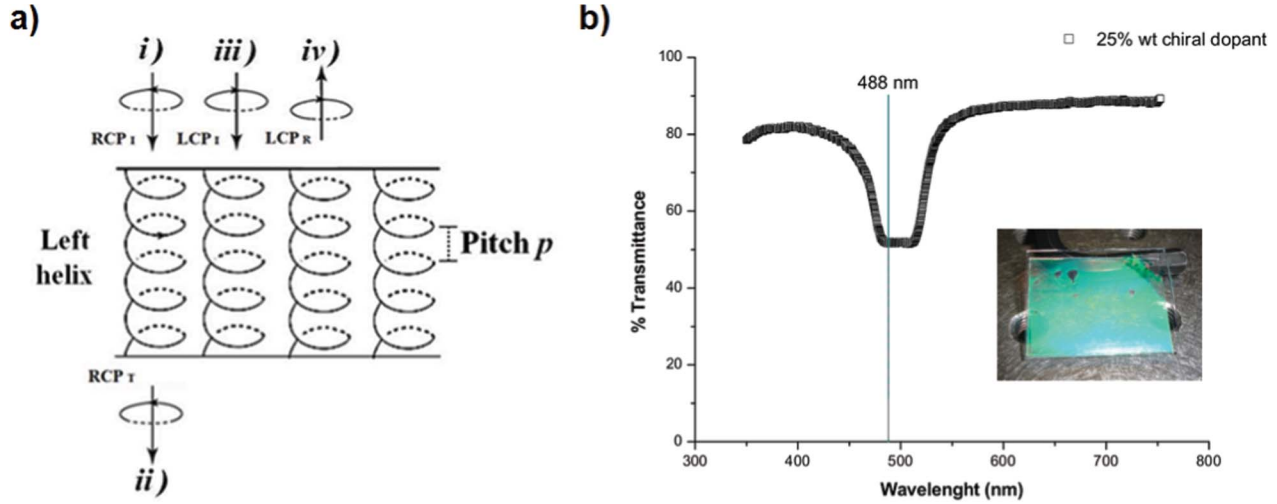

Fig. 1 Bragg reflection and transmission by a film of left-handed CLC in the planar texture. 1a) (*i*) The incident right circular polarized light (RCP) is transmitted through the left cholesteric helix; the transmitted light (*ii*) goes out practically unchanged. In (*iii*) an incident left circular polarized light (LCP) impinges on the sample and the reflected wave (*iv*) is an image of the cholesteric helix with LCP, translated upwards. 1b) Transmission spectrum of a polymerized CLC film between two glass substrates with planar texture for linearly polarized light, the vertical line shows the value of 488 nm, corresponding to the wavelength of the optical tweezers beam.

polarizers, shown in Fig. 2b and 2c, makes evidence of an optical anisotropy of the droplet. The observations in reflection mode,[38] showing conical or equatorial selective reflection, suggest that the helicoidal structures with axes almost perpendicular to the droplets surface are preserved only in some regions inside the particle. Two types of anisotropic organization of the helical structures have been recognized: a conical configuration,[36] depicted in Fig. 2e and a cylindrical one, where the radial helical structure originating from the centre of the microsphere with helicoidal axes perpendicular to the surface is present only at an equatorial region,[36] as reported in Fig. 2f and ref. 38.

The LC droplets are stable, preserving their internal structure during the experiment. The polymerization of the CLC droplets was performed using an UV lamp with an intensity of about 2 $mWcm^{-2}$ and emission centred at 350 nm. UV curing lasted for 6 h under dry nitrogen flux. The configurations of Fig. 2, were fully preserved in the polymeric particles, as already reported.[38]

In order to study the optical manipulation of both chiral isotropic and anisotropic particles, fluid and solid, in water, we employed a standard optical tweezers trap consisting of circularly polarized light with wavelength in the selective reflection band of our CLC (see Fig. 1b). The experimental

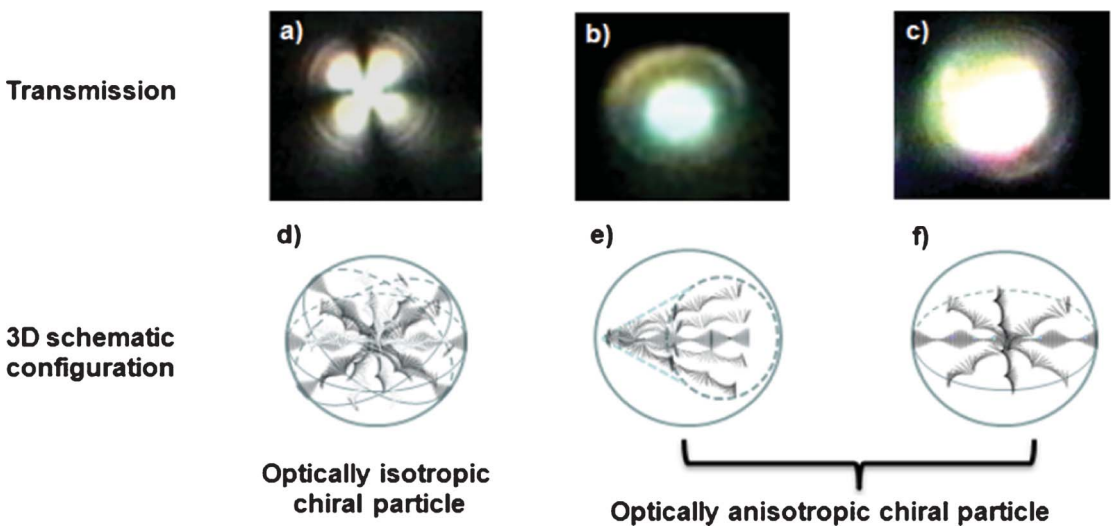

Fig. 2 CLC droplets with short pitch. In the top row are shown microscopic images taken in transmission view through crossed polarizers: a) optically isotropic (radial), b) and c) optically anisotropic. The bottom row shows the 3D schematic configuration of the helicoidal structures, d) optically isotropic (radial), e) and f) optically anisotropic.

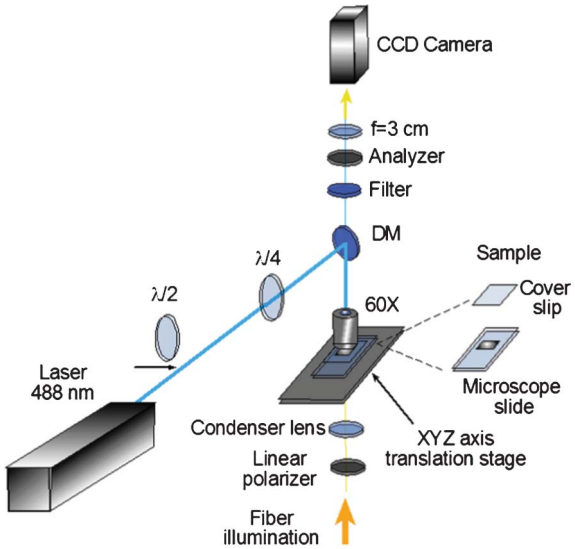

Fig. 3 Experimental setup.

setup is depicted in Fig. 3. An argon ion laser beam at wavelength $\lambda = 488$ nm, linearly polarized along the horizontal direction and with power of $\sim$100 mW, was directed towards a $60\times$ microscope objective (numerical aperture = 0.85) by a dichroic mirror (DM) to focus the beam onto a sample chamber containing the chiral particles dispersed in water.

To change the polarization state of the light beam from linear to circular, a quarter-wave plate ($\lambda/4$) with its axis oriented at 45° is placed before the objective. The insertion of a half-wave plate ($\lambda/2$) before the quarter-wave plate makes it possible to switch from left to right circularly polarized light (LCP and RCP). The sample was placed between a polarizer and an analyzer; it was illuminated with a white light fibre and imaged onto a charge-coupled device (CCD) camera. The sample position was adjusted using a precision three-axis translation stage. We recorded the behaviour of the radial and conical chiral particles (fluid and solid) and investigated their dynamics depending on the handedness of the circular polarization of the trapping beam. The results are described next.

3. Results and discussion

In the case of microspheres with radial configuration (Fig. 2a and 2d), we observe a contrasting behaviour of the same particle, either attractive or repulsive with respect to the optical trap, by switching the polarization from RCP to LCP, respectively (Fig. 4 and Movie 1, 2†). Although surprising, this unique dynamical behaviour can be explained by taking into account the selective reflection of the CLC, the radial configuration of the helical axes inside the particle and the experimental geometry of the optical trap.

While the study of the light propagation in CLC is generally complex, the simple case of propagation nearly along the helical axis, in the Bragg regime, has been deeply studied and described in several papers and books.[23,42] The selective reflection band at oblique incidence undergoes a blue-shift, ranging from few to tens of nanometers depending on the angle.[43] However, as long as the wavelength of the laser remains within the stop-band, a deviation from the normal

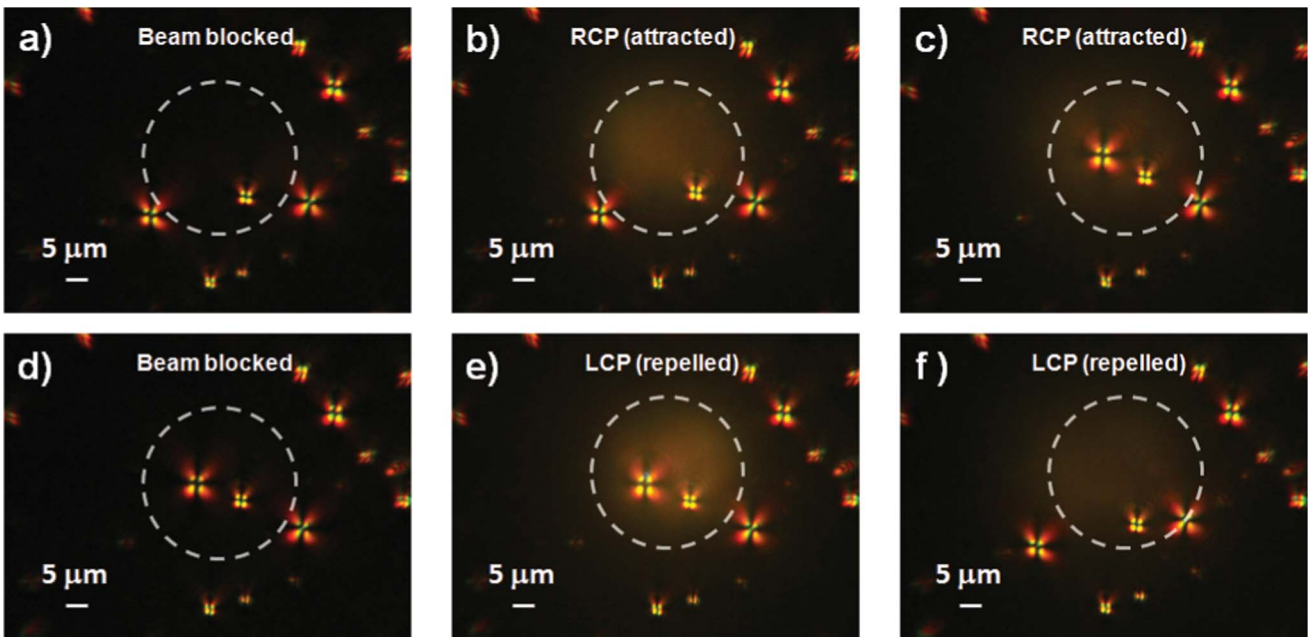

Fig. 4 Radial isotropic CLC droplets between crossed polarizers. a) Laser blocked with particles at rest, with the beam on in b) and c) the particles are attracted towards the centre of the beam spot (dashed circle) for RCP. d) Blocking the beam and switching to LCP, when the beam is on again in e) and f) the particles are repelled from the spot. e) A blue-green dot appears near the centre of the particle. (Movie 1 and 2† are sped up by a factor of 2).

incidence condition, even of some tens of degrees, gives rise to a nearly constant refractive index for circularly polarized waves.[23] In our experiment, due to the geometry of the radial particles, we can consider this condition satisfied by most of the light rays impinging on the sphere. In addition, since the sizes of the spherical particles are well above the wavelength of the trapping beam, a ray optics model[44] will be adopted to describe the qualitative behaviour of the optical trap and to evaluate the net optical force for both circular polarizations.

Under this approach, the light beam is decomposed into individual rays that propagate in straight lines in the media. Each light ray reflects and refracts at the particle-fluid interface according to Snell's law, with reflection and transmission amplitudes proportional to the average Fresnel coefficients. The linear momentum change between the incident ray and the reflected or refracted one is summed over all the incident rays and weighted according with the incident intensity distribution to evaluate the total force on the particle. This net force can be divided into two contributions. One is the scattering force, which is locally directed along the propagation direction and, in general, has the net effect of pushing the particle along the propagation axis. The other is the gradient force, which has its origin in the spatial variations of the light intensity.[2] The effect of the gradient force strongly depends on the properties of the particle. For instance, transparent particles whose refractive index is higher than that of the surrounding medium are attracted towards the maximum intensity regions, whereas highly reflective particles are repelled from those regions, as we shall see next.

In our experimental conditions, as the trapping beam is focused with a relatively low N.A., we can consider that the scattering force is directed vertically downwards, which is the propagation direction, while the gradient force is basically transversal, *i.e.* in the horizontal plane. In the ray optics approach, the equation to obtain the transversal gradient force exerted by the light beam onto the spherical particle of radius R_0, located at the point (x_0, y_0) in a plane z = const, can be written as:

$$F_g(x_0,y_0)=\frac{n_m R_0^2}{c}\int_0^{\frac{\pi}{2}}\int_0^{2\pi} I(x,y,z)\cos\theta\left[R\sin(2\theta) - T^2\frac{\sin(2\theta-2\eta)+R\sin(2\theta)}{1+R^2+2R\cos(2\eta)}\right]\cos\varphi\sin\theta\,d\varphi\,d\theta, \quad (3)$$

where $I(x,y,z)$ is the intensity distribution of the Gaussian beam, n_m is the refractive index of the host medium (water) and (θ, φ) are the polar and azimuthal angles, respectively, in spherical coordinates. The integration is performed over the illuminated hemisphere of the particle. In this case, θ coincides with the incidence angle at each point on the sphere's surface and η is the refraction angle. Note that for radial particles, θ is also the angle between the incident ray and the axis of the helical supramolecular structures. The coordinates of each point on the particle's surface, (R_0, φ, θ), and the position of the centre of the particle with respect to the beam axis, (x_0, y_0, z_0), are related by means of $x = x_0 + R_0\cos\varphi\sin\theta$, $y = y_0 + R_0\sin\varphi\sin\theta$, $z = z_0 + R_0\cos\theta$, with z_0 fixed in eqn (3). Due to symmetry considerations, we can look only at the force along the x direction without loss of generality.

On the other hand, the scattering force along the z axis (x_0 = 0, y_0 = 0) can be evaluated from:

$$F_s(z_0)=\frac{n_m R_0^2}{c}\int_0^{\frac{\pi}{2}}\int_0^{2\pi} I(x,y,z)\cos\theta\left[1+R\cos(2\theta) - T^2\frac{\cos(2\theta-2\eta)+R\cos(2\theta)}{1+R^2+2R\cos(2\eta)}\right]\sin\theta\,d\varphi\,d\theta, \quad (4)$$

where T and R are the transmittance and the reflectance, respectively, derived from the Fresnel coefficients. As we mentioned before, for circularly polarized waves with wavelength inside the stop-band of the CLC these coefficients and the wave propagation depend strongly on the light handedness with respect to the cholesteric helix handedness.[23,42]

Therefore, following our initial hypothesis, in our microparticles having a CLC left-handed helix, we can suppose that the RCP light propagates with a constant average refractive index $\bar{n} = (n_{//} + n_\perp)/2$, according to the eqn (1).[23] Using the values $n_{//}$ = 1.68 and $n_\perp$ = 1.53 of the reactive mesogen, the average refractive index and the refraction angle can be evaluated. Then, to account for the circular polarization, the value of R can be calculated using eqn (5) as the average over the two orthogonal polarization directions respect to the incidence plane at each point:

$$R=\frac{1}{2}\left(\frac{\sin^2(\theta-\eta)}{\sin^2(\theta+\eta)}+\frac{\tan^2(\theta-\eta)}{\tan^2(\theta+\eta)}\right). \quad (5)$$

Since the absorption of the liquid crystal at the considered wavelength is negligible, the transmittance T can be easily evaluated from $T = 1 - R$. These values are included in eqn (3) and (4) to calculate the optical forces, F_g and F_s.

The plots of the forces as a function of the distance from the trap focusing along the transversal and longitudinal directions are shown respectively, in Fig. 5a and 5b. According to our calculations, the expected optical forces predict a trapping of the particle towards the beam axis. The predicted effect is the same observed in the images reported in Fig. 4a–4c: the attractive force in the transversal plane aggregates the radial particles towards the focal spot of the light beam with RCP. The radial particles are identified by their typical cross pattern between crossed polarizers. Therefore, in spite of the complex supramolecular structure of the particle, where linear and circular birefringences are present at the mesoscopic scale, due to the Bragg regime, the mechanical effect of the RCP optical tweezers is the same as the attraction of an optically isotropic and homogenous dielectric sphere with a refractive index higher than that of the surrounding medium.

Nevertheless, by changing the circularly polarized light from right- to left-handed, we observe that the same particles

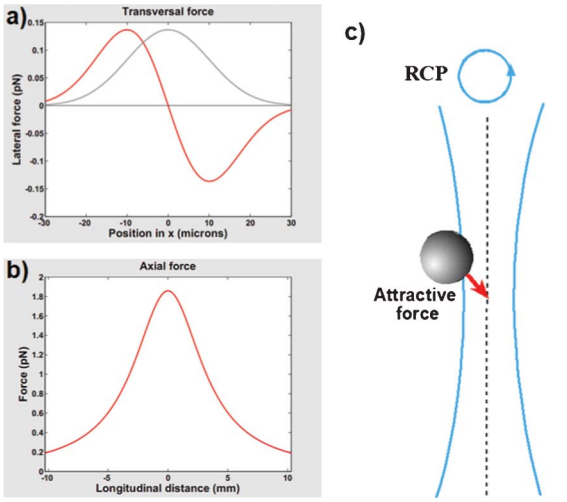

Fig. 5 Forces for right circular polarization. a) Transverse force on the particle (red line) indicates a stable trap, the centre of transversal light intensity distribution (grey profile) correspond to the equilibrium point at $x = 0$. b) Longitudinal force along the axis of propagation of the incident beam. c) Representation of the attractive force toward the beam axis. The parameters of the plots are: ω_0 = 20 μm, R_0 = 2.5 μm, λ_0 = 488nm and P = 100 mW.

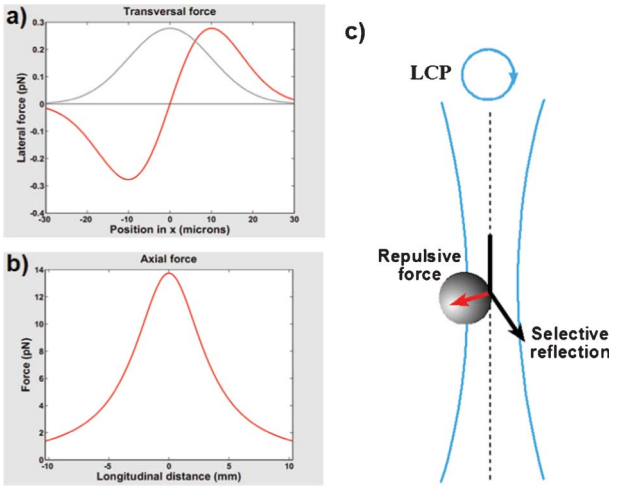

Fig. 6 Forces for left circular polarization. a) Transverse force on the particle (red line) indicates an unstable trap, the centre of transversal light intensity distribution (gray profile) correspond to the unstable equilibrium point at $x = 0$. b) Longitudinal force along the axis of propagation of the incident beam. Notice that the repulsive optical forces are higher in magnitude compared with the case of attractive forces. c) Representation of the repulsive force pulling the particle away from the beam axis. The parameters of the plots are: ω_0 = 20 μm, R_0 = 2.5 μm, λ_0 = 488nm and P = 100 mW.

exhibit a strong reflection and a repulsive force dominates, pushing them outside the illuminated region, Fig. 4e and f. For light with opposite (left) handedness, the propagation in the CLC Bragg regime is interdicted for waves with wavelength inside the stop-band. The Fresnel reflection coefficient near the centre of the stop-band can be now evaluated from the expression reported in ref. 42:

$$r = \tanh(\beta d) \tag{6}$$

where $\beta = \pi(n_{II}^2 - n_{\perp}^2)\sqrt{2} \Big/ 2\lambda\sqrt{n_{II}^2 + n_{\perp}^2}$ and $d = 2R_0$ is the particle diameter, about 5 μm. The R value can be calculated from eqn (6) ($R = |r^2|$) is about 99.8%, which agrees with the measurements of the transmittance reported in Fig. 1b, where the transmittance of linearly polarized light is about 50%. According to these values for transmittance and reflectance, the gradient and scattering forces have been calculated again using eqn (3) and (4). In Fig. 6a and 6b we report the corresponding plots as a function of the distance from the trap focusing along the transverse and longitudinal directions, respectively.

A repulsive force is predicted, in agreement with the experimental observations. In Fig. 4e and in the Movie 1†, as soon as the light polarization of the laser beam (optical tweezers) turns to left-handed, a blue-green dot can be observed in the centre of the microsphere that is subsequently pushed out from the optical trap. The bright dot observed in the centre of the particle can be easily associated with the selective reflection of laser light. This observation supports the hypothesis adopted in the evaluation of optical forces, *i.e.*, that for radial particle most of the rays fulfil the Bragg selective reflection.

Importantly, no rotation is observed for particles manipulated with circularly polarized optical tweezers, neither RCP nor LCP. This behaviour demonstrates that the transfer of linear momentum dominates with respect to the spin angular momentum transfer that could be expected due to the linear optical anisotropy of the LC polymer.

On the other hand, optically anisotropic CLC microspheres (fluid or solid) represent indeed more complex objects, due to the asymmetric configurations of the internal architectures at the supramolecular scale. As a consequence, the particles acquire a net birefringence, as shown in Fig. 2b, c. In this case, in fact, we observe rotation of the particles connected to the transfer of spin angular momentum from the circularly polarized light.

For RCP optical trap the light can propagate everywhere in the particle, then it is trapped and set in rotation (Movie 3†). However, non-uniform rotation is observed and this motion is different depending on the internal particle architecture. Of course, the non-uniform rotation can be accounted for by an irregular angular momentum transfer due to the asymmetric supramolecular structures of the birefringent material inside the particle, which introduces optical inhomogeneity in the object. For the same reason (the inhomogeneity), the rotational axis does not cross the centre of the sphere.

For left circular polarization the particles behave like Janus particles,[45,46] whose surface has a transparent and reflecting (*i.e.* like metallic) part. When the polarization changes from right to left circular, the rotation sense is reversed, but after a few seconds the particle jumps out of the trap. Depending on the forces, the laser power and also the size of the reflecting surface area, the particle can be attracted to the trap once

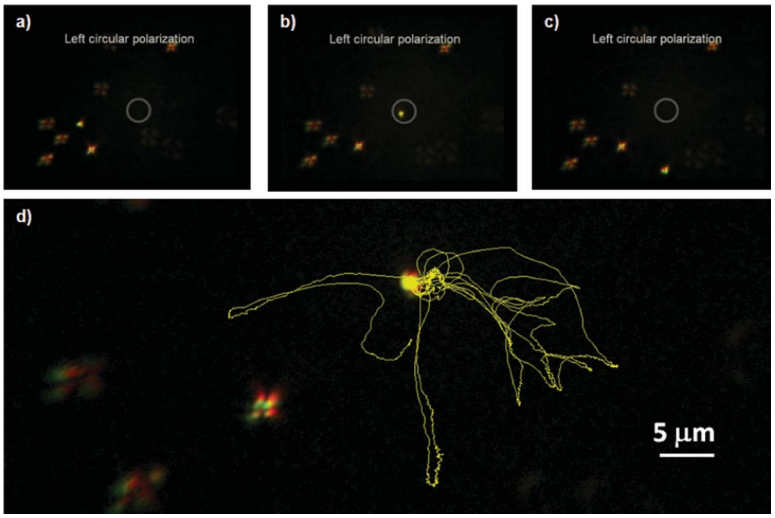

Fig. 7 Attraction and repulsion behaviour of optically anisotropic CLC droplet. a) Optically anisotropic particle repelled from the beam spot (indicated by the circle), b) attraction towards the trap region, c) repulsive force pushing the CLC droplet out of the trap, d) enlarged image with the trajectory described by the particle using Able Particle Tracker software (Movie 4† is sped up by a factor of 3).

again and so on (see Fig. 7 and Movie 4†), or sometimes is even completely expelled from the beam spot (Movie 5†).

Although in this case the evaluation of both gradient and scattering forces is very complicated and requires a proper modelling for the chiral anisotropic microspheres, the observed dynamical behaviour, shown in Fig. 7, can be explained qualitatively using a ray optics scheme. Fig. 8a illustrates the situation in which the incident light rays, a and b, propagate in directions not parallel to the helical axes inside the conical region; in the scheme, the incident light rays are refracted through the particle and the gradient forces F_a and F_b are applied to the particle due to each ray. This simple ray optics approach make evident the importance of the symmetry of conjugated light rays (a and b) to establish a stable trapping in the transverse plane. In the present situation, the symmetry of this process may be easily broken since it depends on the orientation of the particle with respect to the impinging light rays, whose propagation in the particle is strongly influenced by the non-symmetric and non-homogenous internal configuration (Fig. 8b). Moreover, as we mentioned, due to the net birefringence of the particles with conical or cylindrical configuration (Fig. 2b, c, e and f), transfer of spin angular momentum occurs, inducing also a torque on the particle that begins to rotate thereby changing its orientation with respect to the impinging light rays. Depending on the particle position and orientation, some rays could not propagate in the particle;

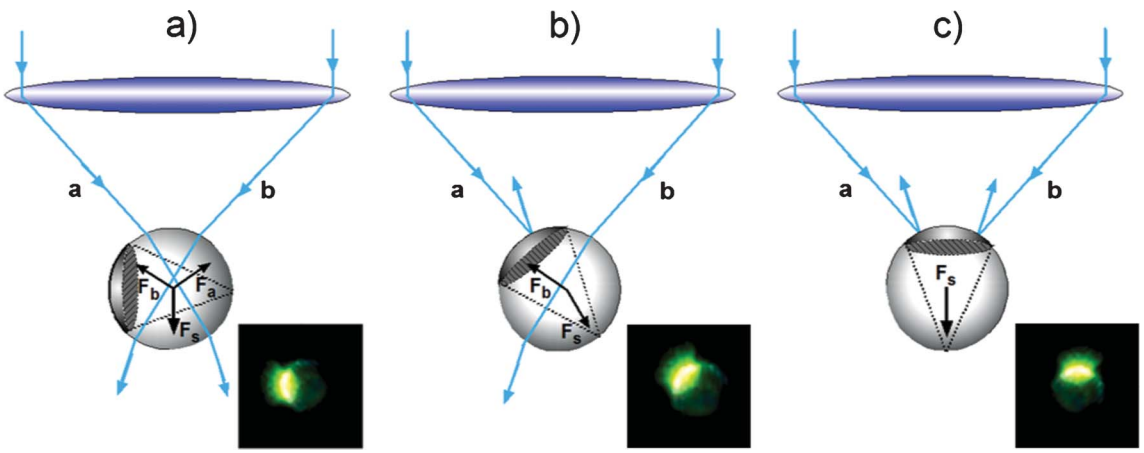

Fig. 8 Qualitative representation of a pair of light rays impinging on an optically anisotropic particle with different orientations, and the consequent optical forces exerted by these rays. a) The rays refract symmetrically inside the particle and thus there is a balance of forces in the transverse plane resulting in a stable optical trap. b) The case of broken symmetry on forces and torque, depending on the orientation and position of the particle with respect to the optical trap. c) The extreme situation when the reflecting part of the surface is oriented such that the incident light is reflected and the particle is repelled due to the scattering force. Insets show the microscope images of the solid CLC sphere with optically anisotropic structure in reflection mode.

this breaks the symmetry, leading to unbalanced torques and forces. The trap becomes unstable and when most of the rays are reflected, Fig. 8b and 8c, the unbalance between the gradient and scattering forces pushes the particle out of the trap. The trapping region in this case is not strongly localized and the rotational motion becomes very complex (Fig. 7d).

4. Conclusions and perspectives

Optically controlled dynamical behaviour of chiral fluid and solid microspheres by means of circularly polarized optical tweezers has been investigated. The liquid crystal phase, in fact, enables the creation of a large variety of self-organized chiral microspheres by manipulating their internal architecture using proper chemical dopants in the liquid crystals and in the water emulsion (chiral agent and surfactant). The use of reactive mesogens allows one to obtain solid particles by means of a photopolimerization process, preserving the internal configurations of the LC droplet precursor.

We have observed very different dynamical behaviours connected to the different internal architectures of the particles. Namely, a net attractive or repulsive optical force on the same particle with radial configuration of the internal helical structures (isotropic chiral particle) has been observed, depending on the handedness of the circular polarization of the incident light. The origin of these forces has been explained taking into account the interplay between the internal helical structure of the CLC and the light circular polarization, when the wavelength of the optical tweezers is of the order of the cholesteric spatial periodicity, and thus the light is selectively reflected due to a circular Bragg condition. Reflection and transmission properties of the CLC have been then considered to evaluate the optical gradient and scattering forces. For optically anisotropic particles, in contrast, the dichotomous behaviour related to the selective reflection of the circularly polarized light produces the trapping and a non-uniform rotation of the particle for right-handed polarization, while unbalanced torques and forces induce a complex dynamic when the circular polarization is reversed to left-handed.

The capabilities of these chiral microparticles, here demonstrated by means of optical manipulation experiments, make them good candidates for developing new concepts in materials science, colloidal and photonics systems, micro-lasers, optical control, micro- and optofluidics, microsensors, *etc.*

Moreover, the unique mechanical and manipulation performances of these devices can be certainly improved and exploited by taking into consideration different light field configurations, like complex beams or holographic patterns with proper architectures of the polarization state.[11–16] In addition, the well known high sensitivity of the LCs to the external stimuli, like electric or magnetic fields, suggests the possibility to introduce additional control parameters and combine, for example, the optical control with the electric and magnetic one.[23,24,42,47]

Finally, the already demonstrated photonic capabilities addressed to develop the innovative concept of microlaser systems,[38] could enable them to acquire also an active role in optically controlled microdevices.

Acknowledgements

The authors are extremely grateful to R. Bartolino, P. Pagliusi and C. Provenzano for useful discussions. This work was partially supported by the Cooperation Project of Great Relevance, Italy-Mexico 2011 ''Optical manipulation strategies in soft matter exploiting holographic tweezers with polarization gradient'', Italian Foreign Ministry.

References

1 A. Ashkin, *Phys. Rev. Lett.*, 1970, **24**, 156.
2 A. Ashkin, J. M. Dziedzic, J. E. Bjorkholm and S. Chu, *Opt. Lett.*, 1986, **11**, 288–290.
3 H. Furukawa and I. Yamaguchi, *Opt. Lett.*, 1998, **23**, 216.
4 A. T. O'Neil and M. J. Padgett, *Opt. Commun.*, 2000, **185**, 139.
5 K. Sasaki, M. Koshioka, H. Misawa, N. Kitamura and H. Masuhara, *Appl. Phys. Lett.*, 1992, **60**, 807.
6 S. Sato, Y. Harada and Y. Waseda, *Opt. Lett.*, 1994, **19**, 1807.
7 A. Ashkin and J. M. Dziedzic, *Science*, 1987, **235**, 1517–1520.
8 K. M. Herbert, W. J. Greenleaf and S. M. Block, *Annu. Rev. Biochem.*, 2008, **77**, 149–176.
9 J. R. Moffitt, Y. R. Chemla, S. B. Smith and C. Bustamante, *Annu. Rev. Biochem.*, 2008, **77**, 205–228.
10 A. Ashkin, *Optical Trapping and Manipulation of Neutral Particles Using Lasers*, World Scientific Publishing, New Jersey, 2006.
11 D. G. Grier, *Nature*, 2003, **424**(6950), 810–816.
12 A. Jonáš and P. Zemánek, *Electrophoresis*, 2008, **29**, 4813–4851.
13 D. J. Stevenson, F. Gunn-Moore and K. Dholakia, *J. Biomed. Opt.*, 2010, **15**, 041503.
14 D. G. Grier, *Curr. Opin. Colloid Interface Sci.*, 1997, **2**(3), 264–270.
15 K. Dholakia and T. Čižmár, *Nat. Photonics*, 2011, **5**, 335.
16 M. Padgett and R. Bowman, *Nat. Photonics*, 2011, **5**, 343.
17 D. Psaltis, S. R. Quake and C. Yang, *Nature*, 2006, **442**, 381.
18 C. Monat, P. Domachuk and B. J. Eggleton, *Nat. Photonics*, 2007, **1**, 106.
19 M. L. Juan, M. Righini and R. Quidant, *Nat. Photonics*, 2011, **5**, 349.
20 H. Schmidt and A. R. Hawkins, *Nat. Photonics*, 2011, **5**, 598.
21 X. Fan and I. M. White, *Nat. Photonics*, 2011, **5**, 591.
22 D. Erickson, D. Sinton and D. Psaltis, *Nat. Photonics*, 2011, **5**, 583.
23 P. G. De Gennes and J. Prost, *The Physics of Liquid Crystals*, Oxford Science Publications, Oxford, England, 1995.
24 P. J. Collings, *Liquid Crystal Nature's Delicate Phase of Matter*, Princeton University Press, Princeton, USA, 2002.
25 H. Coles and S. Morris, *Nat. Photonics*, 2010, **4**, 676.

26 L.M. Blinov and R. Bartolino, *Liquid Crystal Microlasers*, Trensworld Research Network, Kerala, India, 2010.
27 I. I. Smalyukh, D. S. Kaputa, A. V. Kachynski, A. N. Kuzmin and P. N. Prasad, *Opt. Express*, 2007, **15**(7), 4359.
28 N. Murazawa, S. Juodkazis and H. Misawa, *J. Phys. D: Appl. Phys.*, 2005, **38**, 2923–2927.
29 S. Juodkazis, M. Shikata, T. Takahashi, S. Matsuo and H. Misawa, *Appl. Phys. Lett.*, 1999, **74**, 3627–3629.
30 S. Juodkazis, S. Matsuo, N. Murazawa, I. Hasegawa and H. Misawa, *Appl. Phys. Lett.*, 2003, **82**(26), 4657–4659.
31 C. Manzo, D. Paparo, L. Marrucci and I. Jánossy, *Phys. Rev. E*, 2006, **73**(5), 051707.
32 T. A. Wood, H. F. Gleeson, M. R. Dickinson and A. J. Wright, *Appl. Phys. Lett.*, 2004, **84**, 4292–4294.
33 N. Ji, M. Liu, J. Zhou and Z. Lin, *Opt. Express*, 2005, **13**, 5192–5204.
34 M. Humar and I. Muševič, *Opt. Express*, 2010, **18**, 26995–27003.
35 G. P. Crawford and S. Zumer, *Liquid Crystals in Complex Geometries*, Taylor and Francis, London, England, 1996.
36 Y. Boulignad and F. Livolant, *J. Phys.*, 1984, **45**, 1899.
37 G. E. Volovik and O. D. Lavrentovich, *Sov. Phys. JETP*, 1983, **58**(6), 1159–1166.
38 G. Cipparrone, A. Mazzulla, A. Pane, R. J. Hernández and R. Bartolino, *Adv. Mater.*, 2011, **23**(48), 5704.
39 B. M. Ross and A. Lakhtakia, *Optik*, 2008, **119**, 7–12.
40 D. V. Guzatov and V. V. Klimov, *Quantum Electron.*, 2011, **41**, 526.
41 Y. Yang, P. D. Brimicombe, N. W. Roberts, M. R. Dickinson, M. Osipov and H. F. Gleeson, *Opt. Express*, 2008, **16**, 6877–6882.
42 P. Yeh and C. Gu, *Optics of Liquid Crystal Displays*, John Wiley & Sons, 1999.
43 Q. Hong, T. X. Wu and S. T. Wu, *Liq. Cryst.*, 2003, **30**, 367.
44 A. Ashkin, *Biophys. J.*, 1992, **61**, 569–582.
45 M. Conradi, M. Zorko and I. Muševič, *Opt. Express*, 2010, **18**, 500.
46 R. M. Erb, N. J. Jeness, R. L. Clark and B. B. Yellen, *Adv. Mater.*, 2009, **21**, 4825.
47 J. A. Reyes and A. Lakhtakia, *Opt. Commun.*, 2006, **259**, 164–173.